Partial exfoliation of layered double hydroxides in DMSO : a route to transparent polymer nanocomposites

AUTHOR(S)

Yan Zhao, W Yang, Y Xue, Xungai Wang, Tong Lin

PUBLICATION DATE

01-01-2011

HANDLE

10536/DRO/DU:30033556

Journal of Materials Chemistry

Cite this: J. Mater. Chem., 2011, 21, 4869

www.rsc.org/materials

PAPER

Partial exfoliation of layered double hydroxides in DMSO: a route to transparent polymer nanocomposites†

Yan Zhao,[a] Weidong Yang,[b] Yuhua Xue,[a] Xungai Wang[a] and Tong Lin*[a]

Received 18th November 2010, Accepted 24th January 2011
DOI: 10.1039/c0jm03975f

Layered double hydroxides (LDHs), either having nitrate counter anions or intercalated with organic molecules, have been for the first time partially exfoliated in dimethyl sulfoxide (DMSO) to form a transparent suspension. Atomic force microscopy (AFM) images showed that both the lateral size and the thickness of the LDH nanoplatelets were decreased after the exfoliation. The organic-LDHs maintained their intercalation characteristics, *i.e.* the thermal stability improvement of the incorporated organic anions, after the exfoliation in DMSO. Transparent ethylene-vinyl alcohol copolymer (EVOH) nanocomposite films containing partially exfoliated LDHs intercalated with UV absorbers were prepared using DMSO as the processing solvent. As the first reported example of a highly transparent LDH/polymer composite, the obtained composite film had a visible light transmittance of 90% (comparable to that of the pure matrix), was flexible and exhibited an excellent UV-shielding capability and thermal stability.

Introduction

Layered double hydroxides (LDHs) are inorganic nanoplatelet materials consisting of stacks of positively charged hydroxide layers with hydrated anions being located between the interlayer galleries for charge balance. The chemical composition of LDHs is broad, and can be expressed by the general formula $[M^{2+}_{1-x}M^{3+}_{x}(OH)_2]A^{n-}_{x/n}\cdot mH_2O$, wherein M^{2+} and M^{3+} are divalent and trivalent metal ions capable of occupying the octahedral positions of the host layers and A^{n-} is the interlayer anion. The positive charge on the hydroxide layer is due to the partial substitution of divalent metal ions with trivalent ones.

In recent years, LDHs have received increasing attention owing to their versatility in hosting a wide range of metal ions in the hydroxide layer and the ability to encapsulate various organic functional anions.[1–3] Several anionic organic molecules such as dyes and UV absorbers have been incorporated into the interlayer gallery of LDHs.[4–8] The properties of the intercalated species can be modulated by the guest–host interactions, and especially their thermal stability can be improved greatly. The UV absorber-intercalated LDH hybrids have been used for developing new sunscreen cosmetics.[7] They have also been used as fillers to improve the UV resistance of polymers.[9,10] Currently, the challenge of using LDHs as fillers for polymer composites lies in the transparency of the composite materials.[11]

More recently, nanosheets with a thickness around 1–5 nm that are exfoliated from LDHs have shown potential in developing functional composites and complicated nanosheet assemblies.[12–14] However, the exfoliation has been severely inhibited by the high charge density of the LDH host layers and the integrated hydrogen-bonding network between the layers. One effective strategy for exfoliating LDHs has been to weaken the inter-layer interaction by modifying the LDHs with organic anions. For instance, Forano *et al.*[15] first reported the exfoliation of a surfactant (dodecyl sulfate)-intercalated LDH in butanol. Exfoliation of surfactant-intercalated LDHs in alcohols[16] or organic solvent such as CCl_4[17] was also reported by other groups. For polymer composite applications, surfactant-intercalated LDHs were directly exfoliated either with the presence of monomers under a shearing condition,[18] or in polymer solutions.[19,20] It was also reported that lactate- or short-chain-alkyl-carboxylate-containing LDHs swelled and exfoliated in water.[21,22]

The presence of the organic anions however prevents further intercalation of functional materials into the exfoliated LDHs. Therefore, direct exfoliation of LDHs without using any organic anions is highly preferred but remains challenging. Sasaki *et al.*[23] and Norby *et al.*[24] have separately reported the exfoliation of LDHs having nitrate counter anions in formamide. Most recently, Kannan *et al.*[25] reported the synthesis of nitrate LDHs by using hexamine hydrolysis and their following exfoliation in water, which resulted in LDH sheets with a thickness in the range of 2–10 nm.

[a]*Centre for Material and Fibre Innovation, Deakin University, Geelong, VIC, 3217, Australia. E-mail: tong.lin@deakin.edu.au; Fax: +61-3-52272539; Tel: +61-3-52271245*
[b]*Division of Materials Science & Engineering, CSIRO, Highett, VIC, 3190, Australia*

† Electronic supplementary information (ESI) available: Elemental analysis, LDH layer number distribution, AFM images, UV-Vis spectra, FTIR, DSC and stress–strain curves. See DOI: 10.1039/c0jm03975f

Here we report on the partial exfoliation of nitrate LDHs in dimethyl sulfoxide (DMSO). Organic-LDHs, *i.e.* LDHs intercalated with functional organic anions, were also found to be able to exfoliate in DMSO to form a transparent suspension. More importantly, after the exfoliation in DMSO, the intercalation characteristics of organic-LDHs were maintained. Therefore, the partially exfoliated LDH nanosheets in DMSO could be used as carriers for biomolecules or as functional fillers for polymer nanocomposites. Herein, organic UV absorber, 2-hydroxy-4-methoxybenzophenone-5-sulfonic acid (HMBS), was chosen as a model functional anion to be incorporated into LDH to prepare a transparent ethylene-vinyl alcohol copolymer (EVOH) composite film (Fig. 1A). The versatile nature of this system enables to overcome the disadvantage of low thermal stability to naked organic UV absorbers and improve the transparency of the final composite. In addition, as an organic/inorganic hybrid, the HMBS-intercalated LDH, does not bear the main drawback to inorganic UV absorbers (*e.g.* TiO_2 and ZnO), *i.e.*, the photocatalytic oxidation effect on the polymer matrix. To the best of our knowledge, this is the first to demonstrate the partial exfoliation of functional molecule-intercalated LDHs with the intercalation characteristic maintained and the formation of a highly transparent LDH/polymer nanocomposite.

Experimental

Preparation

$Mg(NO_3)_2 \cdot 6H_2O$, $Al(NO_3)_3 \cdot 9H_2O$ and ethylene-vinyl alcohol copolymer (EVOH) with a nominal ethylene content of 44 mol% were purchased from Sigma-Aldrich. UV absorber, 2-hydroxy-4-methoxybenzophenone-5-sulfonic acid (HMBS), was obtained from Riedel-de Haën. All chemicals were used as received.

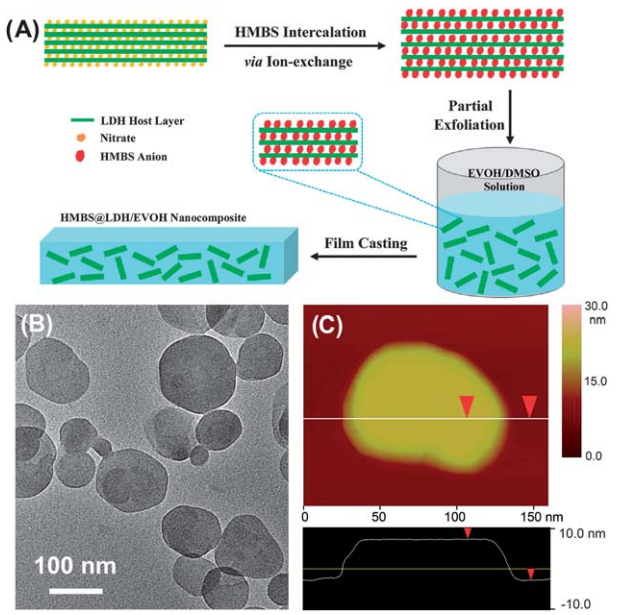

Fig. 1 (A) Schematic illustration of the processes involved in the fabrication of the HMBS@LDH/EVOH composites. (B) TEM and (C) AFM images of the as-synthesized LDHs. The inset in panel C illustrates the height profile along the marked white line.

Synthesis of LDHs. Mg_2Al–NO_3 LDHs (Mg : Al = 2 : 1, mol/mol) were prepared by a previously reported co-precipitation method.[26–28] Briefly, 6.0 mmol $Mg(NO_3)_2 \cdot 6H_2O$ and 3.0 mmol $Al(NO_3)_3 \cdot 9H_2O$ in 20 mL methanol were added into 80 mL NaOH–methanol solution (~0.225 M) with a nitrogen purge. The mixture was then transferred into a Teflon-lined autoclave and aged at 150 °C for 24 h. The resulting slurries were washed several times by repeated centrifugation, and then re-dispersed into CO_2-free water with constant stirring overnight. The elemental analysis and thermogravimetric analysis results (see ESI, Fig. S1†) indicated a composition of $[Mg_2Al(OH)_6]NO_3 \cdot 1.5H_2O$.

Preparation of HMBS-intercalated LDHs (HMBS@LDHs). HMBS was intercalated into the nitrate LDHs by mixing LDHs–water suspension (30 mL, ~0.85 wt%) with 20 mL of HMBS aqueous solution (~32 mmol L^{-1}) for 18 h at room temperature. The pH value of the HMBS solution was adjusted to be about 7 with 1 M NaOH aqueous solution. The obtained solid was washed thoroughly with deionized water by centrifugation.

Exfoliation of LDHs/HMBS@LDHs in DMSO. The centrifuged LDHs/HMBS@LDHs in the wet state were dispersed into DMSO under stirring. To facilitate the exfoliation, the dispersed solution was treated with an ultrasonic bath for 10 min. For comparison, other solvents were also used to disperse the LDHs.

Preparation of HMBS@LDH/EVOH films. The HMBS@LDHs were dispersed into a DMSO solution containing 5 wt% EVOH. The nanocomposite film was prepared by casting the solution on a glass substrate, followed by solvent evaporation in an oven at 95 °C for 3 h.

Physical characterization

Atomic force microscopy (AFM) was performed using a Nanoscope IIIa multimode scanning probe microscope (Digital Instruments) operating in tapping mode. Transmission electron microscopy (TEM) observation was undertaken under JEOL JEM-2100 microscope at an acceleration voltage of 200 kV. Powder X-ray diffraction (XRD) data were collected on a PANalytical X'Pert diffractometer with Cu Kα radiation over the 2θ range of 2–70°. The thickness (L_c) of the LDH crystals was estimated using Scherrer equation: $L_c = K\lambda/(\beta \cos \theta)$, where K is the shape factor (0.9 was set for LDHs),[29,30] λ is the X-ray wavelength (0.154 nm for Cu Kα), β is the full width at half-maximum (fwhm) of the (00*l*) reflection, and θ is the Bragg diffraction angle. UV-Visible spectra were recorded using a Varian Cary 3 spectrophotometer. Fourier transform infrared (FTIR) spectra were recorded with samples in KBr discs on a Bruker VERTEX 70 instrument with a resolution of 4 cm^{-1} accumulating 32 scans. Thermogravimetric (TG) analysis was carried out with a Netzsch STA 409 PC instrument at a heating rate of 10 °C min^{-1} in air. Differential scanning calorimetry (DSC) measurements were conducted on a TA DSC Q200 instrument in a dry nitrogen atmosphere at a heating/cooling rate

of 10 °C min^{-1}. Tensile tests were carried out in a Lloyd LR30K machine with a load cell of 100 N.

Results and discussion

Exfoliation

Fig. 1B shows the typical TEM image of the LDH crystals deposited onto grids from an aqueous dispersion, with the lateral size of *ca.* 50–150 nm. Fig. 1C displays the height profile of an individual platelet, exhibiting a fairly flat terrace with a thickness of 9.8 nm. Based on a large number of AFM images, the thickness distribution of the LDH platelets was determined to be in the range 6.3–15.3 nm. The average thickness estimated by the XRD data was ~13.2 nm. Considering the basal spacing of ~8.96 Å (Fig. 2A), the thickness value suggests that the obtained crystallites contain stacks of up to 15 LDH layers.

As shown in Fig. 3A, the LDH suspension in water is translucent. Treatment of the centrifuged LDH aggregate with DMSO yielded a transparent suspension. The transparency of the LDH suspensions was quantitatively measured using a UV-Vis spectrometer. At 589 nm wavelength, the transmittance of the suspension in DMSO is 90% in contrast to the 36% transmittance for the aqueous suspension. Fig. 3B shows a clear Tyndall light scattering of the LDH suspension in DMSO,

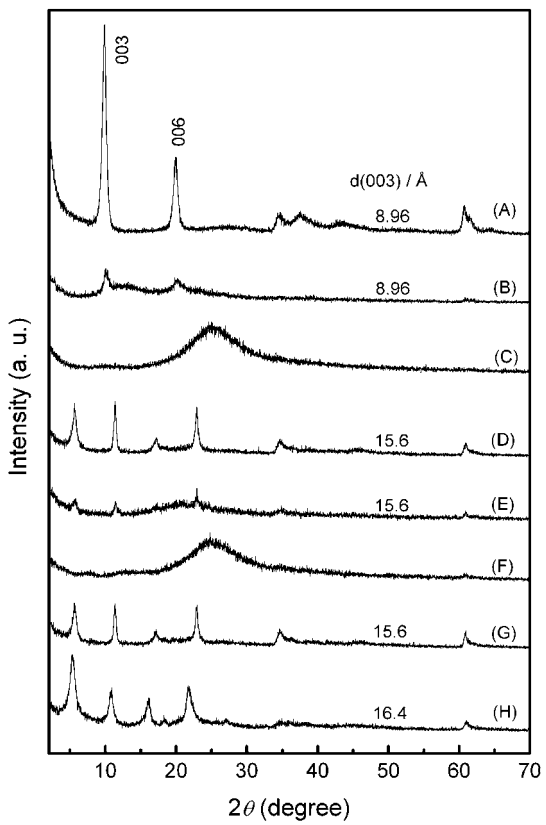

Fig. 2 XRD patterns of (A) untreated LDHs; wet colloidal LDH aggregates centrifuged from (B) DMSO and (C) formamide suspensions; (D) untreated HMBS@LDHs; wet colloidal HMBS@LDH aggregates centrifuged from (E) DMSO and (F) formamide suspensions; dried HMBS@LDH aggregates centrifuged from (G) DMSO and (H) formamide suspensions.

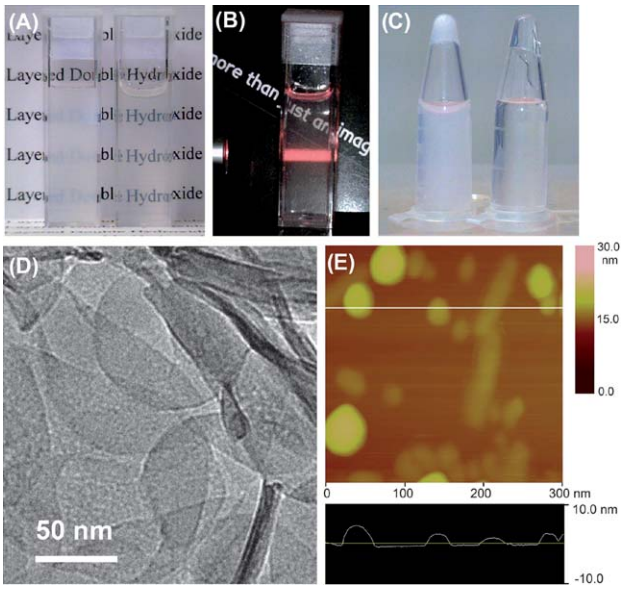

Fig. 3 (A) Photograph of the colloidal suspensions of LDHs in water (left) and DMSO (right). (B) The light beam demonstrating the Tyndall effect of the LDH suspension in DMSO. (C) Photograph of the colloidal LDH aggregates centrifuged from the water (left) and DMSO (right) suspensions. (D) TEM image of the LDHs (DMSO suspension). (E) AFM image of the LDHs (DMSO suspension) and a height profile along the marked white line.

indicating the presence of abundant exfoliated nanosheets. After centrifugation, the aggregate obtained from the aqueous dispersion was opaque. In contrast, the colloidal LDH aggregate from the DMSO suspension was a clear gel (Fig. 3C). The XRD measurement revealed that the resultant wet aggregate from DMSO suspension still exhibited a similar pattern to that of the untreated LDHs (Fig. 2B).

After DMSO treatment, the LDH crystals kept their platelet-like shape, as evidenced by the TEM image shown in Fig. 3D. The change in the thickness of the LDH platelets was monitored by AFM. As shown in Fig. 3E, the height profile indicated that the thickness of the platelets decreased to 5.3, 2.7, 1.8 and 2.7 nm, corresponding to 6, 3, 2 and 3 stacked LDH layers, respectively, which offers the direct evidence of the exfoliation (see the distribution histogram in the ESI, Fig. S2†). Here it should be noted that some irregular fragments appeared after exfoliation, indicating that a breakage or fracture of the platelets occurred during the DMSO exfoliation process. This phenomenon is similar to previous observations reported on delamination of LDHs using formamide.[23]

For comparison, as a general delaminating agent for LDHs, formamide was also used to exfoliate the as-synthesized LDHs. In the transparent formamide suspension, there appeared some exfoliated nanosheets with a thickness of ~0.8 nm (see ESI, Fig. S3†), which corresponded to the thickness of a single LDH layer.[23,31] The XRD pattern of the wet colloidal aggregate centrifuged from the formamide suspension is shown in Fig. 2C. The characteristic basal diffraction peaks of LDHs were absent in this pattern, indicating the disappearance of the layer structure. The pronounced halo in the 2θ range of 20–30° may be due to the scattering of liquid formamide.[31] The average lateral size

of the LDH platelets decreased from 109.8 ± 33.3 nm to 37.7 ± 13.2 nm and 24.4 ± 9.1 nm for DMSO and formamide treatments, respectively (see ESI, Fig. S4†). Other polar solvents including acetone, acetonitrile, tetrahydrofuran (THF), dimethylformamide (DMF), ethanol, and *N*-methylpyrrolidone (NMP) were also tested (see ESI, Fig. S5†). Among these solvents, NMP also led to the formation of transparent LDH suspension. When acetone, acetonitrile, and THF were used, sedimentation occurred just after shaking. For DMF and ethanol, the LDHs flocculated after standing 2 hours.

It is well-known that in the interlayer space of LDHs there is a dense network of hydrogen bonds formed through the interlayer water molecules, which are both hydrogen-bonded to hydroxyl groups of the LDH layers and coordinated to interlayer anionic guests.[32] Formamide was proposed to replace the interlayer water molecules and destruct the strong hydrogen-bonding network, thus inducing the exfoliation.[23,33] In fact, formamide and DMSO have been found to be able to intercalate into layered silicate kaolinite through hydrogen bonding to the hydroxyl surfaces of kaolinite.[34,35] Herein, the exfoliation of LDHs using DMSO and NMP could follow a similar mechanism to that of formamide, presumably because of their strong hydrogen-bonding interaction with the hydroxyl groups of the LDH layers. It was also reported that formamide could slightly dissolve LDHs.[36] Here we examined the Mg and Al contents in the supernatants of the LDH suspensions in formamide and DMSO, and found that the dissolution degree of LDHs in DMSO is much lower than that in formamide (see ESI, Table SI†).

Thermal stability of HMBS

HMBS was intercalated into the nitrate LDHs *via* an ion-exchange reaction.[7,37] The obtained HMBS@LDHs kept the platelet-like shape and the lateral size was comparable to the original LDH crystals (see ESI, Fig. S6†). The HMBS intercalation was confirmed by the change in the UV-Vis and FTIR spectra (see ESI, Fig. S7 and S8†) and XRD pattern (Fig. 2D). To gain insight into the influence of the LDH interlayer on the thermal stability of the intercalated HMBS anions, TG analysis was performed (Fig. 4; see ESI, Fig. S9† for corresponding DSC curves). For naked HMBS molecules, a weight loss was observed at around 100 °C, which was attributed to the evaporation of the physically absorbed water. The main weight loss due to HMBS decomposition occurred between 200 and 400 °C in two very close stages. The TG curves of the LDHs displayed two main weight loss stages. The first one was in the range of 100–220 °C, corresponding to the removal of interlayer water molecules. The second one, between 350 and 550 °C, was contributed to the dehydroxylation of the brucite-like LDH layers and the decomposition of the interlayer nitrate anions. In the case of HMBS@LDH, the loss of the interlayer water exhibited almost the same tendency as that of LDH. At above 350 °C, the dehydroxylation of the layers overlapped with the thermal decomposition of the intercalated HMBS. This suggests that the intercalated HMBS did not decompose until the LDHs broke down, indicating the greatly enhanced thermal stability of HMBS after the intercalation.

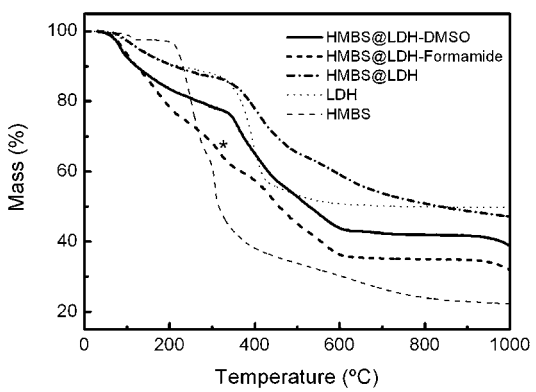

Fig. 4 TG curves of HMBS, LDH, HMBS@LDH (dried from water suspension), HMBS@LDH–DMSO (dried from DMSO suspension), and HMBS@LDH–formamide (dried from formamide suspension).

It was interesting to find that HMBS@LDHs were also able to exfoliate in DMSO and form a transparent suspension. The XRD pattern of the wet aggregate centrifuged from the suspension shows typical basal diffraction peaks, indicating the partial exfoliation of HMBS@LDHs (Fig. 2E). After drying, the resultant powder showed almost the same XRD profile with that of the untreated HMBS@LDHs (Fig. 2G). Here it should be pointed out that the exfoliation of HMBS@LDHs in DMSO did not deteriorate the thermal stability of the intercalated HMBS molecules (Fig. 4). For comparison, the effect of formamide treatment on HMBS stability was also studied. After the exfoliation in formamide, there appeared a weight loss around 310 °C, which corresponded to the HMBS decomposition (Fig. 4). XRD study shows that the basal spacing of HMBS@LDHs was increased from 15.6 to 16.4 Å after formamide treatment (Fig. 2H), which may be due to the rearrangement of the HMBS molecules or the incorporation of formamide molecules into the interlayers. Therefore, unlike the exfoliation in formamide, the partial exfoliation of organic-LDHs in DMSO favors maintaining the host–guest interaction characteristics, and the LDH interlayers can still provide effective protection for the intercalated HMBS.

Transparent nanocomposites

HMBS@LDH/EVOH composite films were fabricated by a solution-casting method. When the HMBS@LDHs were dispersed in a DMSO solution containing 5 wt% EVOH, visually transparent suspensions were formed at all HMBS@LDH solid concentrations investigated (Fig. 5A). The thin films cast from the suspensions were flexible and optically transparent (Fig. 5B and C). As shown in Fig. 5D, the composite films exhibited an increased UV absorption (<400 nm) and the absorption intensity in the UV region increased with the increase in the HMBS@LDH loading, reaching a UV absorption of as high as 95% when the HMBS@LDH composition was 10 wt%. Meanwhile, the composite films kept a transmittance higher than 90% in the visible region, being almost the same as that of the pure EVOH film. For comparison, we also prepared HMBS@LDH/EVOH composite films using *N*,*N*-dimethylacetamide (DMAc) as the processing solvent, in which the HMBS@LDHs were not exfoliated. For the composite film containing 15 wt%

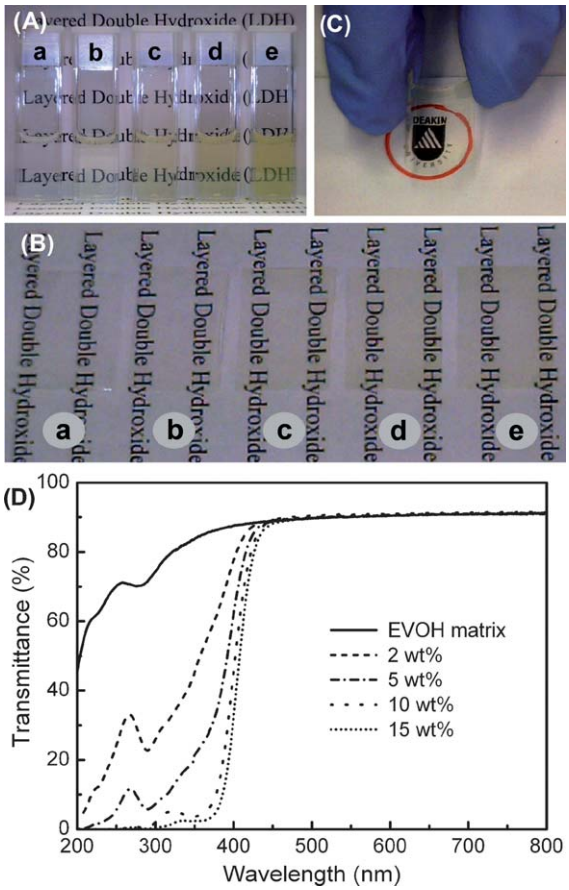

Fig. 5 Photographs of (A) EVOH–DMSO solutions (EVOH, 5 wt%) containing (a) 0, (b) 2, (c) 5, (d) 10, and (e) 15 wt% HMBS@LDH solid concentrations, respectively; (B) HMBS@LDH/EVOH composite films cast from the solutions shown in panel A; and (C) an HMBS@LDH/EVOH film with 15 wt% HMBS@LDHs. (D) UV-Vis transmission spectra of EVOH and HMBS@LDH/EVOH composite films with different HMBS@LDH compositions.

unexfoliated HMBS@LDHs, the average transmittance (450–800 nm) was only 67% (see ESI, Fig. S10†).

Fig. 6 shows the TEM images of pure EVOH and HMBS@LDH/EVOH nanocomposites containing 2, 5, 10, and 15 wt% HMBS@LDHs, respectively. The HMBS@LDH platelets were dispersed homogeneously in the EVOH matrix without aggregation, which guaranteed the high transparency. Usually, to realize the homogeneous distribution of inorganic fillers in the polymeric matrix, the surface functionalization of the fillers to generate chemical or physical interactions with the polymer matrix is critical.[38] In our system here, the LDHs bear abundant hydroxyl groups and interlayer HMBS anions. As a control, the LDHs without HMBS intercalation were incorporated into EVOH to prepare an LDH/EVOH composite film, which is highly transparent also. This suggests that the homogeneous distribution of LDHs did not derive from the intercalation of HMBS. It is known that EVOH contains a hydroxyl group in each unit. We found that the EVOH solution in DMSO containing HMBS@LDHs formed viscous gels (see ESI, Fig. S11†) after several days to weeks depending on the composition of HMBS@LDHs. This gelation behavior implied the formation of

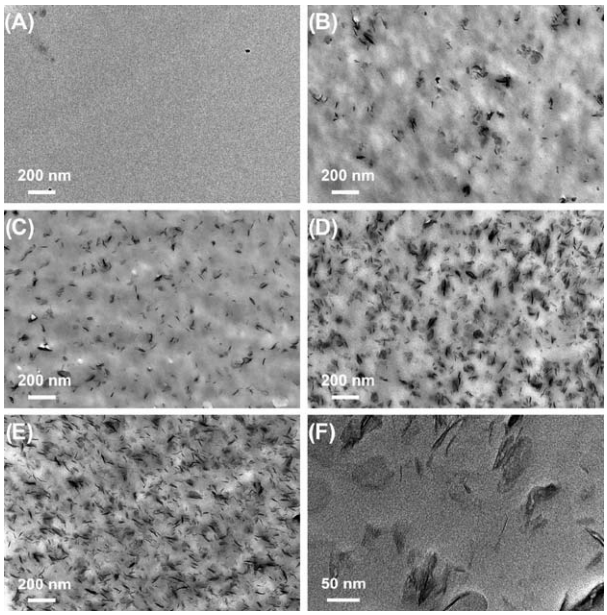

Fig. 6 TEM images of HMBS@LDH/EVOH nanocomposite films with the HMBS@LDH compositions of (A) 0 wt%, (B) 2 wt%, (C) 5 wt%, (D) 10 wt%, and (E and F) 15 wt%.

physically crosslinked network, which presumably resulted from the hydrogen bonding interaction between the LDHs and the EVOH chains. In this case, the LDH platelets could act as crosslinking sites using surface hydroxyl groups, contributing to their homogeneous dispersion.

The thermal behavior of HMBS@LDH/EVOH composites was examined using DSC (see ESI, Fig. S12†). The glass transition temperatures (T_g) did not show significant difference between them. Compared with the pure EVOH, the composite films had a slight decreased melting temperature (T_m), which can be ascribed to the decrease in EVOH crystallinity. A similar phenomenon was also observed for montmorillonite/EVOH composites.[39]

The mechanical property of the HMBS@LDH/EVOH films was studied by measuring the stress–strain curves (see ESI, Fig. S13†). Pure EVOH film showed a typical behavior of plastic materials with significant yielding. The presence of HMBS@LDHs led to the decrease in the breaking elongation of the composite films. With increasing the HMBS@LDH loading, the Young's modulus and the tensile strength of the composite films were increased; for instance, the tensile strength increased from 25.6 MPa for the pure EVOH film to 30.7 and 46.5 MPa for the composite films containing 2 wt% and 15 wt% HMBS@LDHs, respectively. The enhanced mechanical property of the composite films can be ascribed to the hydrogen bonding interaction between LDHs and the EVOH matrix.

Conclusions

We have demonstrated that LDHs with nitrate counter anions can be exfoliated in DMSO. The AFM results showed the LDHs were partially delaminated and stacks of LDH layers with different thicknesses were obtained. An organic UV absorber (HMBS) was intercalated into LDHs. TG analysis confirmed

that the intercalated HMBS had a considerably increased thermal stability. Such an improvement was attributed to the electrostatic interaction between the guest HMBS anions and the host LDH layers. After the HMBS-intercalated LDHs were exfoliated in DMSO, the host–guest intercalation characteristic was still maintained. Based on the exfoliation of LDHs in DMSO, we have prepared transparent EVOH composite films using a solution-processing method. When HMBS was taken as the model functional anion, the composite films showed an excellent UV-shielding capability, but were highly transparent to visible light. This work paves the way for the use of LDHs not only as nanofillers for transparent polymer composites but also as protective-carriers for organic functional molecules.

Acknowledgements

Financial support from Deakin University under Alfred Deakin Postdoctoral Research Fellowship scheme is acknowledged.

References

1 A. I. Khan and D. O'Hare, *J. Mater. Chem.*, 2002, **12**, 3191.
2 F. Leroux and C. Taviot-Gueho, *J. Mater. Chem.*, 2005, **15**, 3628.
3 G. R. Williams, T. G. Dunbar, A. J. Beer, A. M. Fogg and D. O'Hare, *J. Mater. Chem.*, 2006, **16**, 1222.
4 Y. J. Feng, D. Q. Li, Y. Wang, D. G. Evans and X. Duan, *Polym. Degrad. Stab.*, 2006, **91**, 789.
5 Q. He, S. Yin and T. Sato, *J. Phys. Chem. Solids*, 2004, **65**, 395.
6 S. Mandal, D. Tichit, D. A. Lerner and N. Marcotte, *Langmuir*, 2009, **25**, 10980.
7 L. Perioli, M. Nocchetti, V. Ambrogi, L. Latterini, C. Rossi and U. Costantino, *Microporous Mesoporous Mater.*, 2008, **107**, 180.
8 X. R. Wang, J. Lu, W. Y. Shi, F. Li, M. Wei, D. G. Evans and X. Duan, *Langmuir*, 2010, **26**, 1247.
9 G. J. Cui, X. Y. Xu, Y. J. Lin, D. G. Evans and D. Q. Li, *Ind. Eng. Chem. Res.*, 2010, **49**, 448.
10 D. Q. Li, Z. J. Tuo, D. G. Evans and X. Duan, *J. Solid State Chem.*, 2006, **179**, 3114.
11 C. Nyambo, P. Songtipya, E. Manias, M. M. Jimenez-Gasco and C. A. Wilkie, *J. Mater. Chem.*, 2008, **18**, 4827.
12 R. Z. Ma, Z. P. Liu, L. Li, N. Iyi and T. Sasaki, *J. Mater. Chem.*, 2006, **16**, 3809.
13 J. B. Liang, R. Z. Ma, N. B. O. Iyi, Y. Ebina, K. Takada and T. Sasaki, *Chem. Mater.*, 2010, **22**, 371.
14 Z. P. Liu, R. Z. Ma, Y. Ebina, N. Iyi, K. Takada and T. Sasaki, *Langmuir*, 2007, **23**, 861.
15 M. Adachi-Pagano, C. Forano and J. P. Besse, *Chem. Commun.*, 2000, 91.
16 B. R. Venugopal, C. Shivakumara and M. Rajamathi, *J. Colloid Interface Sci.*, 2006, **294**, 234.
17 M. Jobbagy and A. E. Regazzoni, *J. Colloid Interface Sci.*, 2004, **275**, 345.
18 S. O'Leary, D. O'Hare and G. Seeley, *Chem. Commun.*, 2002, 1506.
19 W. Chen, L. Feng and B. J. Qu, *Chem. Mater.*, 2004, **16**, 368.
20 W. Chen and B. J. Qu, *Chem. Mater.*, 2003, **15**, 3208.
21 T. Hibino and M. Kobayashi, *J. Mater. Chem.*, 2005, **15**, 653.
22 N. Iyi, Y. Ebina and T. Sasaki, *Langmuir*, 2008, **24**, 5591.
23 L. Li, R. Z. Ma, Y. Ebina, N. Iyi and T. Sasaki, *Chem. Mater.*, 2005, **17**, 4386.
24 Q. L. Wu, A. Olafsen, O. B. Vistad, J. Roots and P. Norby, *J. Mater. Chem.*, 2005, **15**, 4695.
25 C. A. Antonyraj, P. Koilraj and S. Kannan, *Chem. Commun.*, 2010, **46**, 1902.
26 E. Gardner, K. M. Huntoon and T. J. Pinnavaia, *Adv. Mater.*, 2001, **13**, 1263.
27 J. A. Gursky, S. D. Blough, C. Luna, C. Gomez, A. N. Luevano and E. A. Gardner, *J. Am. Chem. Soc.*, 2006, **128**, 8376.
28 P. Gunawan and R. Xu, *Chem. Mater.*, 2009, **21**, 781.
29 P. Benito, M. Herrero, C. Barriga, F. M. Labajos and V. Rives, *Inorg. Chem.*, 2008, **47**, 5453.
30 S. K. Sharma, P. K. Kushwaha, V. K. Srivastava, S. D. Bhatt and R. V. Jasra, *Ind. Eng. Chem. Res.*, 2007, **46**, 4856.
31 Z. P. Liu, R. Z. Ma, M. Osada, N. Iyi, Y. Ebina, K. Takada and T. Sasaki, *J. Am. Chem. Soc.*, 2006, **128**, 4872.
32 J. W. Wang, A. G. Kalinichev, J. E. Amonette and R. J. Kirkpatrick, *Am. Mineral.*, 2003, **88**, 398.
33 T. Hibino, *Chem. Mater.*, 2004, **16**, 5482.
34 R. L. Frost, J. Kristof, E. Horvath and J. T. Kloprogge, *J. Phys. Chem. A*, 1999, **103**, 9654.
35 S. Letaief and C. Detellier, *J. Mater. Chem.*, 2005, **15**, 4734.
36 C. R. Gordijo, V. R. L. Constantino and D. D. Silva, *J. Solid State Chem.*, 2007, **180**, 1967.
37 K. R. Franklin, E. Lee and C. C. Nunn, *J. Mater. Chem.*, 1995, **5**, 565.
38 S. H. Stelzig, M. Mapper and K. Muellen, *Adv. Mater.*, 2008, **20**, 929.
39 N. Artzi, Y. Nir, M. Narkis and A. Siegmann, *J. Polym. Sci., Part B: Polym. Phys.*, 2002, **40**, 1741.

